ISSN 2504-9593
DOI: 10.5281/zenodo.18755074
https://ijree.com/index.php/publications/article/view/34
Int. J. Renew. Energ & Environ Vol.4 (1), pp 72-89(2026)

IMPACT OF ADDITION OF TITANIUM DIOXIDE (TiO_2) NANO PARTICLE ON THE DIELECTRIC PROPERTIES OF BIODIESEL EXTRACTED FROM JATROPHA OIL

[1]Auwalu Inusa Abubakar, [2]Ogah Matthew Ogobeche, [3]Auwal Muhammad, [3]Sunusi Abdulmalik Aliyu

[1 & 3]Department of Physics, Faculty of Science, Aliko Dangote University of Science and Technology, Wudil

[2]Department of Physics Education, School of Secondary Education, (Science), Federal College of Education (Technical), Bichi

[3]Department of physics, Rabi'u Musa kwankwaso College of Advance and Remedial studies Tudun wada Dankade Kano. Nigeria.

Corresponding author: ogobeche@gmail.com; 08033212246

Abstract

Vegetable oils are gaining increasing attention as sustainable substitutes for conventional mineral oils in electrical insulation applications due to their biodegradability, renewability, and favorable thermal characteristics. Among these alternatives, *Jatropha curcas* oil has demonstrated promising dielectric properties, particularly adequate electrical breakdown strength for high-voltage applications. However, there remains limited understanding of the dielectric behavior of Jatropha biodiesel modified with metal oxide nanoparticles, as most existing studies focus on crude or refined oils and employ narrow or unsystematic nanoparticle loadings, with insufficient correlation between structural characteristics and dielectric performance. In this study, the effect of titanium dioxide (TiO_2) nanoparticle incorporation on the dielectric properties of biodiesel derived from purified *Jatropha curcas* oil was systematically investigated. The crude oil was first purified and transesterified to obtain biodiesel, after which TiO_2 nanoparticles were dispersed at concentrations ranging from 0.1 wt.% to 0.5 wt.% in increments of 0.1 wt.%. Structural, elemental, and molecular characterizations of the crude oil, biodiesel, and nanoparticle-modified samples were conducted using Scanning Electron Microscopy (SEM), X-ray Diffraction (XRD), X-ray Fluorescence (XRF), and Fourier Transform Infrared Spectroscopy (FTIR). Dielectric parameters, including dielectric constant (ε'), dielectric loss (ε''), and dissipation factor ($\tan\delta$), were measured over a range of temperatures using a digital LCR meter. The results demonstrate that the incorporation of TiO_2 nanoparticles significantly enhances the dielectric performance of Jatropha biodiesel by reducing dielectric losses and improving polarization stability. These findings highlight the potential of TiO_2-modified Jatropha biodiesel as an environmentally friendly and high-performance insulating fluid for high-voltage and high-temperature electrical applications.

Keywords: Biodiesel, Vegetable oil, Jatropha oil, Titanium Dioxide (TiO_2)

1. Introduction

Power transformers are indispensable components of modern electrical power systems, enabling efficient transmission and distribution of alternating-current (AC) electricity. Their operational reliability depends largely on the condition of the insulation system, which typically consists of cellulose-based paper impregnated with insulating oil that provides both electrical insulation and cooling (Saha, 2003). Over time, mineral oil–paper insulation systems deteriorate under combined thermal, electrical, and chemical stresses, leading to

reduced dielectric strength, mechanical degradation, and eventual shortening of transformer service life (Prevost and Oommen, 2006). Consequently, continuous improvement and proper selection of insulating liquids are essential for ensuring safe and reliable transformer operation (Yuan *et al.,* 2023).

Dielectric liquids have been used in transformers for decades because they provide electrical insulation, facilitate heat dissipation, and suppress electrical arcing (Wang *et al.,* 2012; Boyekong *et al.,* 2021). Mineral oil remains the most widely applied insulating fluid due to its favorable dielectric strength, low viscosity, and effective cooling capability (Navas *et al.,* 2012; Wang & Tang, 2018; Tlhabologo *et al.,* 2021). The cooling performance of transformer oil is governed by key thermophysical properties, including viscosity, thermal conductivity, specific heat capacity, density, and thermal expansion coefficient, which collectively influence oil circulation and heat-transfer efficiency (Wang & Tang, 2018; Nadolny, 2024). While improved thermal conductivity and heat capacity enhance hot-spot cooling, unfavorable changes in viscosity or flow behavior can reduce convective heat transfer and elevate operating temperatures (Deenesh *et al.,* 2021).

Despite its technical advantages, mineral oil presents significant environmental and safety concerns. Its fossil-based origin, poor biodegradability, and relatively low flash and fire points pose risks of environmental contamination and fire hazards during leakage, spillage, or fault conditions (Manish *et al.,* 2021; Nogueira *et al.,* 2022). These limitations have intensified research into alternative insulating fluids that offer improved environmental sustainability and fire safety without compromising electrical performance. Natural and synthetic ester-based oils have emerged as promising substitutes because they are biodegradable, derived from renewable sources, and exhibit higher flash and fire points than mineral oil (Nogueira *et al.,* 2022; Méndez *et al.,* 2024). Transformer retrofilling studies and mixed-oil investigations further demonstrate that natural esters can deliver acceptable dielectric and thermal performance alongside enhanced fire safety, supporting their application in existing transformer fleets (Wang *et al.,* 2022; Karaman *et al.,* 2023; McShane *et al.,* 2023). Broader reviews also identify ester-based oils and nanofluids as viable solutions to the environmental drawbacks of conventional mineral oil (Jacob *et al.,* 2020; Olmo *et al.,* 2022; Siddique *et al.,* 2025).

Growing ecological awareness has further driven interest in vegetable-oil-based biodiesels as transformer insulating fluids. These oils are biodegradable, exhibit high flash points, and possess favorable lubrication and dielectric properties (Karthik *et al.,* 2022). Common natural ester sources include rapeseed, soybean, sunflower, palm, and *Jatropha curcas*. Among these, *Jatropha curcas* oil is particularly attractive because it is non-edible, can be cultivated on marginal land, and has a fatty-acid composition well suited for dielectric applications (Mahlia *et al.,* 2020). Nevertheless, biodiesel-based insulating fluids may suffer from elevated dielectric losses and limited thermal-oxidation stability, which can restrict their long-term performance in high-voltage environments.

To address these limitations, nanotechnology has been increasingly explored as a means of enhancing the electrical and thermal performance of insulating fluids. Siddique *et al.,* (2025) developed a nanofluid by blending three vegetable oils castor, flaxseed, and blackseed into a novel base fluid that

outperformed all other samples evaluated, thereby demonstrating superior performance characteristics. The findings confirm the strong potential of natural ester–based vegetable oil nanofluids as viable and sustainable alternatives, attributable to their favorable intrinsic properties and the environmentally benign synthesis approach employed. The addition of metal-oxide nanoparticles such as TiO_2, ZnO, and Al_2O_3 has been shown to improve dielectric strength, suppress dielectric losses, and modify polarization and charge-transport mechanisms in insulating liquids (Soudagar *et al.,* 2021; Daniel *et al.,* 2024). Among these additives, titanium dioxide (TiO_2) nanoparticles are particularly promising due to their high permittivity, excellent dielectric strength, thermal stability, and chemical inertness. However, most existing studies focus on crude or refined vegetable oils, apply limited or non-systematic nanoparticle concentrations, and rarely establish a clear relationship between nanoparticle-induced structural characteristics and temperature-dependent dielectric behavior (Sudhakar *et al.,* 2024; Widagdo *et al.,* 2025). In view of these research gaps, the present study investigates the impact of TiO_2 nanoparticle addition on the dielectric properties of biodiesel extracted from *Jatropha curcas* oil. Biodiesel is first produced from Jatropha oil and subsequently modified with finely incremented TiO_2 nanoparticle loadings. The study evaluates how nanoparticle incorporation influences key dielectric parameters over a range of operating temperatures, while correlating microstructural, elemental, and molecular characteristics with observed electrical behavior. Through this systematic approach, the work seeks to clarify the mechanisms by which TiO_2 nanoparticles enhance polarization stability and reduce dielectric losses without chemically altering the biodiesel matrix, thereby contributing to the development of environmentally friendly nanofluid insulating systems for high-voltage transformer applications.

2. Materials and Methods

2.1 Materials

Crude *Jatropha curcas* oil obtained from local sources was used as the feedstock for biodiesel production. Analytical-grade methanol served as the alcohol reagent, while Sulfuric acid (H_2SO_4) and sodium hydroxide (NaOH) pellets were employed as the acid and base catalysts, respectively, in the two-step transesterification process. Commercial Titanium Dioxide (TiO_2) nanoparticles with particle sizes below 100 nm and a purity greater than 99% were utilized as a heterogeneous catalyst and additive. Distilled water was used during the washing and purification stages to remove residual impurities.

2.2 Biodiesel production

Biodiesel used in this study was produced from *Jatropha curcas* oil using a widely adopted two-step transesterification process to accommodate the relatively high free fatty acid (FFA) content commonly found in crude Jatropha oil. (1) acid-catalyzed esterification to reduce free fatty acids (FFA) below 1% (H_2SO_4, methanol), followed by (2) base-catalyzed transesterification (NaOH, methanol) to convert triglycerides to fatty acid methyl esters (FAME). Reaction conditions (molar ratios, temperatures, reaction times) followed optimized laboratory practice; separation and washing procedures ensured removal of glycerol and residues. The two-step approach acid esterification to reduce FFA followed by base-catalyzed methanolysis minimizes soap formation, improves catalyst efficiency and

yields, and is well documented for non-edible feedstocks (Farouk, 2024).

2.2.1 Feedstock pretreatment and purification

Crude Jatropha oil was first heated to ~100–110 °C under mild vacuum or dry heat to remove entrained water and volatile impurities, then filtered to remove particulates and solid debris. Moisture removal is critical because water promotes saponification and lowers biodiesel yield (Osman, 2024). Degumming (hot-water treatment / centrifugation) was performed where necessary to remove phospholipids and gums that can interfere with catalyst performance (Maniam, 2023; Osman, 2024).

2.2.2 Acid esterification (FFA reduction)

Because high FFA (>1–2%) causes saponification during base transesterification, a pre-esterification step using an acid catalyst (typically H_2SO_4 at 0.5–1.0 wt.% of oil) and excess methanol (molar ratios commonly 6:1–12:1) was performed at 60 °C for 1 hour to convert FFAs to methyl esters (Farouk, 2024; Ahmed, 2024). The reaction mixture was allowed to settle and the aqueous/acidic phase (containing converted FFA by-products) was separated prior to the base step. This procedure follows best practices summarized in recent transesterification reviews.

2.2.3 Base-catalyzed transesterification (main conversion)

Following FFA reduction to <1%, the pretreated oil underwent base-catalyzed transesterification using NaOH (typical loadings 0.5–1.5 wt.% relative to oil) with methanol (commonly 6:1 molar ratio) at 60 °C under vigorous stirring for 1 hour. Reaction conditions (molar ratio, catalyst concentration, temperature and time) were chosen in accordance with kinetic and optimization studies to achieve high conversion while limiting side reactions (Jain, 2010; Farouk, 2024). After reaction, the mixture was allowed to separate; the denser glycerol-rich bottom layer was drained to yield crude biodiesel on top.

2.2.4 Phase separation, washing and purification

The crude biodiesel layer contains residual methanol, catalyst salts, unreacted glycerides and soaps; these impurities must be removed to meet fuel standards. Traditional wet-washing (sequential warm water washes, often including an acidified first wash to neutralize residual alkali) effectively removes water-soluble contaminants, methanol and catalyst residues (Osman, 2024; Jariah *et al.,* 2021). However, to reduce wastewater generation and process costs, dry-washing using adsorbents (e.g., magnesol, ion-exchange resins, or bio-adsorbents such as sawdust) or membrane techniques have been proposed and demonstrated as effective alternatives (Arenas, 2021; Atadashi *et al.,* 2015). The selection of washing/drying protocol must ensure residual water <500 ppm and low glycerol/soap levels to avoid interference with downstream nanoparticle dispersion and dielectric testing.

2.2.5 Drying and final conditioning

After washing, biodiesel was dried (e.g., gentle heating at 80–110 °C and/or vacuum drying) to remove dissolved and entrained water; Karl-Fischer titration or Coulometric moisture measurement are recommended to verify water content (Fregolente *et al.,* 2015). Drying is essential prior to any nanoparticle dispersion because moisture elevates dielectric loss and can catalyse degradation

during storage. Alternative moisture removal strategies such as adsorption with molecular sieves or hydrophilic hydrogels have also been validated in the literature.

2.2.6 Rationale for the chosen protocol and quality control

The combined two-step transesterification and careful purification/drying protocol was selected to (a) maximize FAME conversion and biodiesel yield, (b) minimize residual catalyst and soap, and (c) produce a low-water, low-ionic-contaminant biodiesel suitable for reproducible dielectric characterization. These steps conform to established practice and industry guidance (Farouk, 2024; Osman, 2024), and were validated by routine quality checks (acid value, kinematic viscosity, density, residual methanol and water content) following ASTM/EN standard test methods prior to nanoparticle dosing and dielectric measurements.

2.3 TiO_2 Doping Procedure

TiO_2 nanoparticles were added as a heterogeneous catalyst / additive at concentrations of 0.0, 0.1, 0.2, 0.3, 0.4 and 0.5 wt.% relative to oil mass. The nanoparticles were dispersed by magnetic stirring and brief ultrasonication prior to transesterification (two-step process), and doped biodiesel samples were prepared for physicochemical testing after phase separation and drying.

2.4 Characterization

FTIR, XRD, SEM: TiO_2 nanoparticle phase and morphology were characterized by XRD and SEM; FTIR confirmed functional groups and interaction signatures for crude, purified and TiO_2-doped biodiesel.

2.5 Dielectric Measurements

The dielectric characterization of the biodiesel samples both pure and TiO_2-doped was conducted to evaluate the influence of nanoparticle concentration on the electrical insulating behavior of Jatropha biodiesel. Three key dielectric parameters were examined: dielectric constant (ε') obtained from eqn 2, dielectric loss (ε'') from eqn 1, and dissipation factor ($\tan \delta$) measured directly from the LCR meter. These parameters are critical indicators of the fluid's ability to store electrical energy, resist dielectric heating, and minimize conductive or polarization losses. The measurements were performed using a precision Digital LCR Meter equipped with temperature control and frequency-sweep capabilities.

2.5.1 Instrumentation and Measurement Setup

A digital LCR meter (typically operating in the frequency range of 100 Hz–1 MHz) was used due to its high accuracy in impedance-based dielectric testing. The LCR meter was connected to a parallel-plate liquid dielectric test cell, consisting of:

- Two stainless-steel electrodes (circular, polished)
- A fixed electrode spacing (typically 2–4 mm)
- A thermostatic jacket around the test cell for temperature regulation

The test cell constant was obtained from the manufacturer and cross-validated using standard calibration fluids. The biodiesel samples were preconditioned and maintained within the desired temperature using a circulating water bath with ±0.1 °C stability to ensure reproducibility. Temperature points tested were 20 °C, 40 °C, 60 °C, 80 °C, and 100 °C.

2.5.2 Calibration Procedure

Before measurements, the LCR meter and test cell were calibrated using:

1. Open-circuit calibration – to compensate for stray capacitance.
2. Short-circuit calibration – to account for lead inductances and plate resistance.
3. Standard dielectric fluid validation – typically transformer mineral oil with known ε′ and tan δ values was used to confirm system accuracy.

Calibration was repeated after every set of samples or anytime temperature drift was detected.

2.5.3 Sample Preparation for Measurement

Each biodiesel sample (0.0–0.5 wt.% TiO_2) was:

1. Thoroughly homogenized using an ultrasonic bath for 5–10 minutes to minimize nanoparticle sedimentation.
2. Degassed under mild vacuum to remove trapped air bubbles that could distort dielectric readings.
3. Injected carefully into the test cell to avoid air entrapment.

The samples were allowed to thermally equilibrate for about 10 minutes at each temperature before measurement.

2.5.4 Measurement Procedure

Dielectric parameters were obtained using the LCR meter in capacitance (Cp) and dissipation factor (D) mode because:

- ε′ is directly related to capacitance
- tan δ is directly measured as the dissipation factor
- ε″ is derived from:

$$\varepsilon'' = \varepsilon' \cdot tan\ \delta$$

1

For each sample, measurements were taken at multiple frequencies (100 Hz–1 MHz), but results at 1 kHz were used as the primary reference because this frequency is widely adopted in transformer liquid diagnostics.

The dielectric constant was calculated using:

$$\boldsymbol{\varepsilon}' = \frac{C_p.d}{\boldsymbol{\varepsilon}_0.A}$$

2

Where:

- C_p: measured capacitance
- d: electrode gap
- A: electrode area
- $\boldsymbol{\varepsilon}_0$: permittivity of free space

Data for each temperature-frequency point were recorded in triplicate, and the average value was used to minimize instrumental and environmental errors.

2.5.5 Rationale for Dielectric Testing Method

The chosen measurement technique is consistent with transformer insulation fluid standards such as:

- IEC 60247 (Measurement of relative permittivity, dielectric dissipation factor, and DC resistivity of insulating liquids)
- ASTM D150 (AC loss characteristics and permittivity)

Measuring ε′, ε″, and tan δ provides insight into:

- Polarization behavior (interfacial and dipolar)
- Energy storage capability
- Insulation losses under AC stress
- Effectiveness of TiO_2 as dielectric enhancement additive

Because dielectric properties are highly sensitive to temperature and moisture, analytical conditions were tightly controlled.

2.5.6 Consideration for Nanoparticle Stability

Nanoparticle-based dielectric fluids may show:

- Agglomeration
- Sedimentation
- Interfacial polarization effects

Thus, immediate testing after dispersion and maintaining mild agitation before measurement ensure that dielectric readings reflect the true behavior of a stable nanoenhanced biodiesel system.

3. Results

3.1 Characterization of the samples

3.1.1 XRF of TiO_2

Table 1 below shows the XRF elemental percentage concentration of TiO_2, based on the result TiO_2 has the highest elemental composition of 93.8% followed by MgO 0.81% and Al_2O_3 with the least elemental composition of 0.049%.

Table 1: XRF elemental percentage concentration

Oxide	Percentage Composition (%)
Al_2O_3	0.049
Ni_2O	0.69
CuO	0.04
ZnO	0.317
Ta_2O_5	0.185
Na_2O	0.75
MgO	0.81
TiO_2	93.75
SiO_2	0.2565
P_2O_2	0.8
SO	0.1408
Cl	0.0649
CaO	0.57
TiO	0.032

3.1.2 XRD of TiO_2

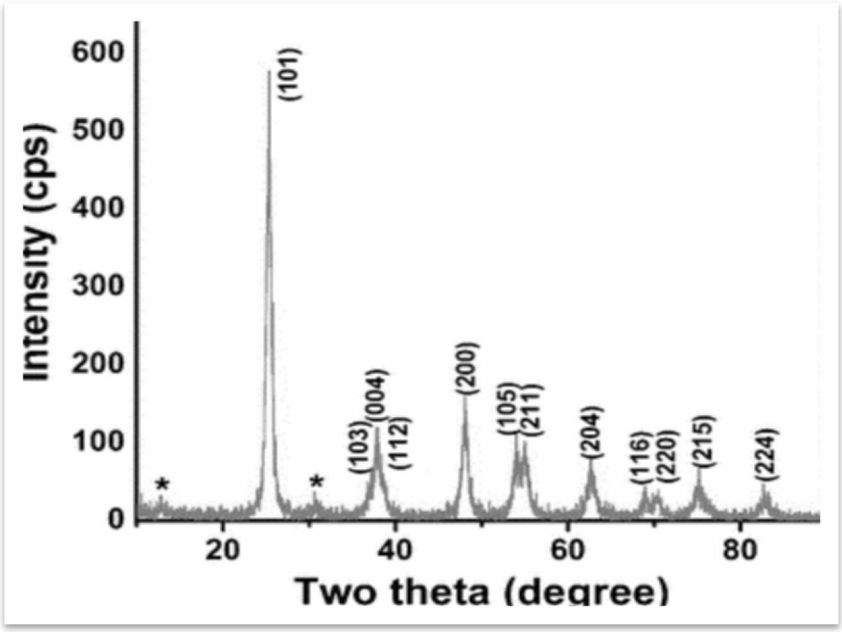

Fig. 1: XRD Pattern of TiO_2 Nanoparticles

The XRD pattern of commercial TiO_2 as shown in Fig. 1 affirms the presence of TiO_2 nanoparticles. The prominent peaks were compared with JCPDS data (PDF No: 21-1272) (anatase TiO_2), and dashed lines were located at $2\theta = 25.30^{o}$, 48.07, and 62.66^{o}, which are the strong diffraction peaks associated with the anatase phase and the peaks obtained in the pattern coincides well with the literature. In the XRD pattern of the TiO_2 nanoparticles, the diffraction peaks corresponding to 2θ values near 25.3° and 48.0° are characteristic of the *anatase* crystalline phase of titanium dioxide. Specifically, the intense peak at approximately $2\theta \approx 25.3°$ can be indexed to the (101) lattice plane**,** while the peak near 48.0° corresponds to the (200) reflection of the anatase structure, as confirmed by comparison with standard TiO_2 diffraction data and recent studies on anatase-phase TiO_2 nanomaterials (Águila-Martínez *et al.,* 2025; Sellami *et al.,* 2025). The high intensity and sharpness of the (101) peak are indicators of good crystallinity and well-ordered lattice planes, since narrow, intense peaks imply large coherent scattering domains and low microstrain within the crystal lattice (Águila-Martínez *et al.,* 2025; Structural and optical characterization of TiO_2 nanoparticles, 2025). Together, these strong, well-defined peaks confirm that the prepared TiO_2 sample predominantly crystallizes in the anatase phase with high structural order and purity. The peaks marked with asterisks (*) represent weak reflections that do not match the characteristic anatase TiO_2 planes and are therefore attributed to minor impurity phases, trace residual precursors, or background/instrumental contributions. The low intensity of these asterisk-marked peaks indicates that such secondary phases are present only in negligible amounts and do not significantly affect the overall crystallinity or phase purity of the TiO_2 nanoparticles.

3.1.3 SEM Analyses of TiO_2

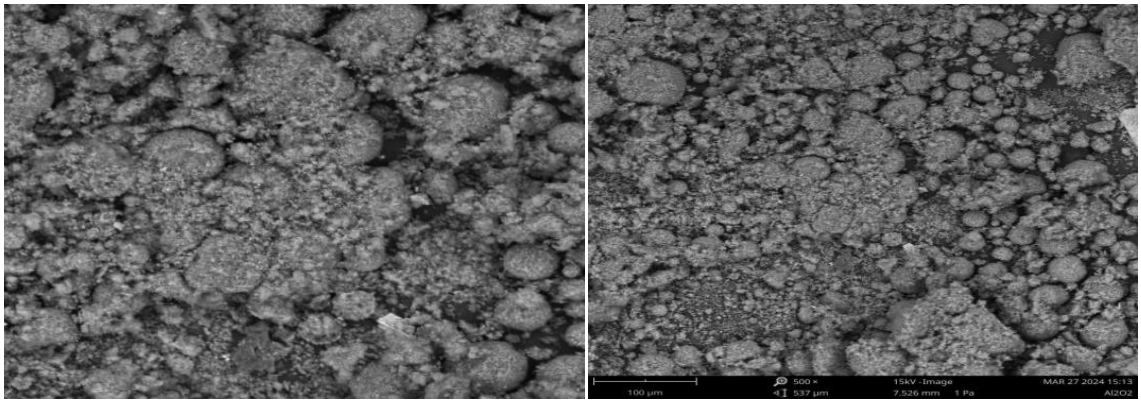

Fig. 2: SEM images of titanium dioxide

Figure 2 shows Scanning Electron Microscope of TiO_2. It indicates the presence of dispersed particles. The SEM micrograph revealed that the particle size of TiO_2 was in the nanometer range. The small particle size of TiO_2 provides a large specific surface area, enhancing the interaction between hydroxyl ions (OH^-) in solution and the TiO_2 surface, which leads to the formation of highly reactive hydroxyl radicals (•OH). These radicals act as strong oxidizing agents and are responsible for the degradation of dye molecules adsorbed on the TiO_2 surface. Morphological analysis further indicates that TiO_2 nanoparticles are typically spherical, smooth, and uniformly distributed, forming a homogeneous catalyst structure without irregular surface features (Fujishima *et al.,* 2008; Hoffmann *et al.,* 1995).

3.1.4 FTIR SPECTRA

3.1.4.1 FTIR of TiO_2

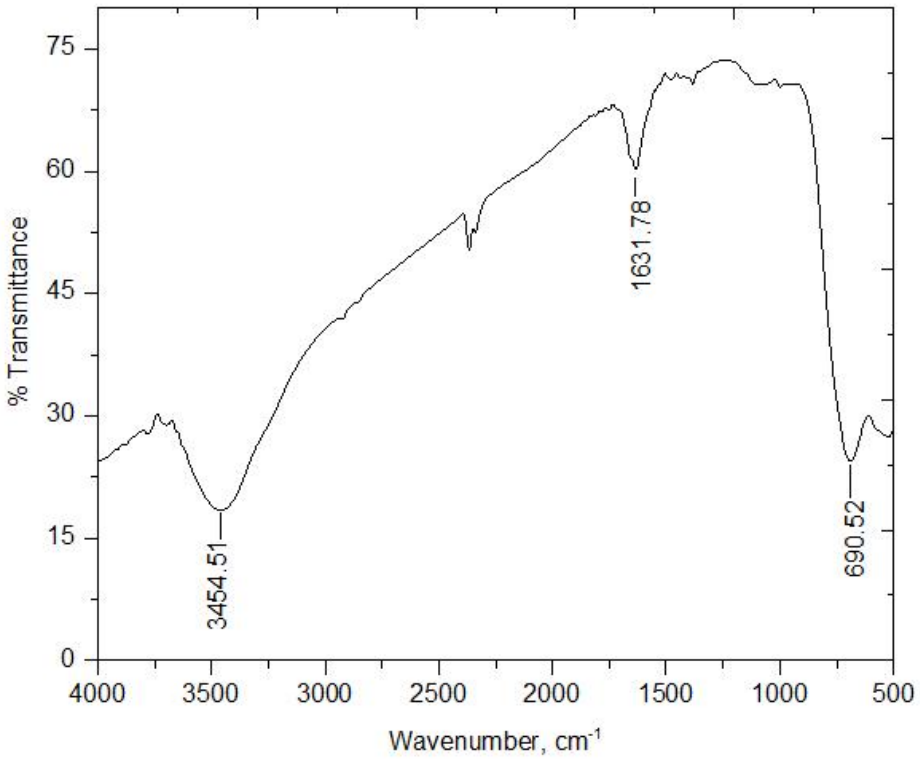

Fig 3: FTIR spectrum of TiO_2

The FTIR spectrum of TiO_2 exhibited several characteristic absorption bands, as shown in Fig. 3. The broad band observed at approximately 3454 cm^{-1} corresponds to the O–H stretching vibration, while the band around 1632 cm^{-1} is attributed to the O–H bending vibration of physically adsorbed water molecules, indicating the presence of surface hydroxyl groups. The strong absorption band near 690 cm^{-1} is assigned to Ti–O stretching vibrations, which are characteristic of titanium dioxide and confirm the formation of the TiO_2 structure (Nakamoto, 2009).

3.1.4.2 FTIR of crude Jatropha oil

The presence of ester fatty acid in a carboxyl group was justified by employing FTIR on Jatropha seed oil.

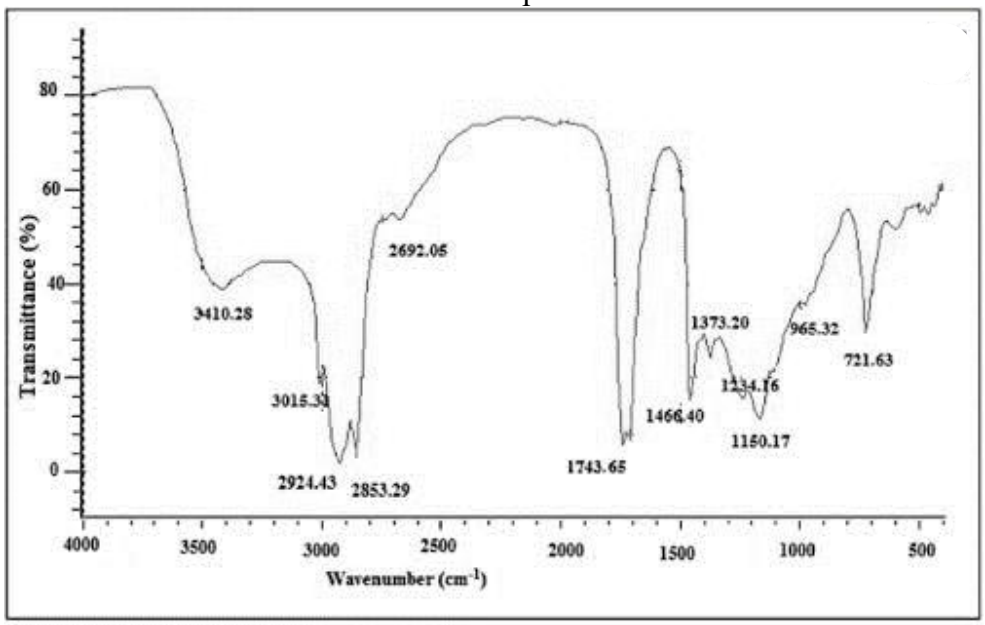

Fig. 4: FTIR of crude Jatropha Oil

The broad O–H stretch around 3470 cm^{-1} suggests the presence of moisture or minor free fatty acids in crude oil, which is typical before purification. A prominent peak near 1745 cm^{-1} corresponds to the C=O stretch of ester linkages in triglycerides, confirming that the oil is rich in triacylglycerols. Peaks between 2925 and 2854 cm^{-1} are indicative of $–CH_2–$ groups, reflecting the long-chain fatty acid components that dominate vegetable oils. The presence of alkene groups (C=C) is confirmed by the weak absorption near 3010 cm^{-1}, indicative of unsaturated fatty acids like oleic and linoleic acid. The strong ester (C=O and C–O) signals suggest the oil is a good feedstock for transesterification due to the high triglyceride content. Presence of unsaturation (C=C) also impacts oxidative stability and cold flow properties, which are important parameters for biodiesel quality. The absence of significant free fatty acid peaks (which typically appear near 1700–1710 cm^{-1} for carboxylic acids) indicates a relatively low FFA content**,** reducing the risk of soap formation during base-catalyzed transesterification.

FTIR Analysis of Purified and TiO_2-Doped Jatropha Oil

FTIR spectroscopy was further employed to analyze the chemical transformations that occurred during the purification and

nanoparticle doping of Jatropha oil. The comparison of spectra before and after purification, and following TiO_2 nanoparticle addition, reveals subtle but important chemical changes relevant to the biodiesel production process.

FTIR Spectrum of Purified Jatropha Oil

Purification of crude Jatropha oil typically involves degumming, neutralization, and sometimes bleaching to remove gums, free fatty acids (FFAs), and other impurities. This refining process alters the FTIR profile slightly, especially in regions associated with hydroxyl and carboxyl groups. A reduction in the broad O–H peak (compared to crude oil) indicates successful removal of water and FFAs. The C=O ester peak remains strong, confirming that the triglyceride structure is intact. The absence of FFA-associated carboxylic acid peaks (around 1708 cm^{-1}) suggests that neutralization was effective. The purified oil is chemically stable and compositionally suitable for transesterification without risk of excessive soap formation.

FTIR Spectrum of TiO_2 Doped Jatropha Oil

When TiO_2 nanoparticles are added to purified Jatropha oil, physical interactions and potential weak chemical interactions between the TiO_2 surface and polar functional groups in the oil can result in noticeable spectral changes. However, since TiO_2 acts primarily as a catalyst and is chemically stable, the FTIR spectrum of the doped oil remains similar with a few key differences. A weak Ti–O–C signal may appear in the fingerprint region (500–600 cm^{-1}), suggesting possible interaction between TiO_2 and ester/carboxyl groups**.** Slight shift in the carbonyl (C=O) peak indicates weak coordination or adsorption on the TiO_2 surface. The overall ester structure remains intact**,** confirming that TiO_2 does not chemically degrade the oil but may aid in activation during transesterification.

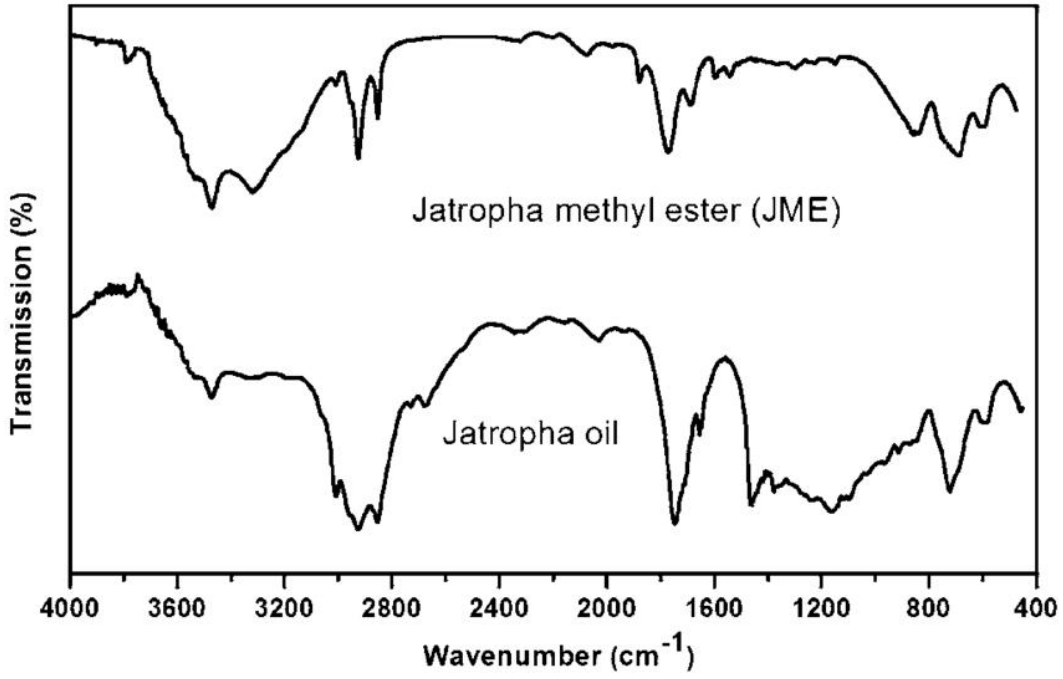

Fig 5: FTIR Analysis of crude and purified jatropha oil

Purification reduces unwanted polar components (like FFAs and water), leading to a cleaner and more defined FTIR spectrum. TiO_2 doping does not chemically alter the

core structure of the oil but shows weak physical interactions with biodiesel functional groups, consistent with the behavior of supported metal oxide nanoparticles (Qamar *et al.,* 2023). These interactions may occur via surface adsorption mechanisms without disrupting triglyceride integrity. This explains why TiO_2 can act as an effective heterogeneous catalyst, enhancing reactivity and reaction performance. For example, biodiesel production performance has been shown to improve when TiO_2-based nanocatalysts are used, with enhanced conversion and kinetics relative to conventional catalysts (Hanif *et al.,* 2023).

FTIR analysis of purified and TiO_2 doped Jatropha oil demonstrates that the essential triglyceride structure is retained through processing. The purification step improves the chemical clarity of the oil, while TiO_2 doping introduces subtle physical interactions that enhance catalytic performance during transesterification. These observations confirm the chemical readiness and compatibility of the oil for biodiesel production.

3. Results and Discussion

3.1 Dielectric Constant (ε′)

The dielectric constant (ε′) indicates the ability of a material to store electrical energy when subjected to an alternating electric field. For biodiesel-based insulating fluids, a higher ε′ value supports improved charge storage, enhanced polarization, and stronger insulating performance in high-voltage equipment. Fig. 6 presents the dielectric constant of pure and TiO_2-doped Jatropha biodiesel measured at temperatures ranging from 20 °C to 100 °C and nanoparticle concentrations between 0.0 and 0.5 wt.%.

A clear trend is observed: ε′ increases with both temperature and TiO_2 nanoparticle loading. The rise with temperature is attributed to enhanced thermal agitation that facilitates dipole orientation and improves dielectric polarization. Similarly, TiO_2 nanoparticles enhance ε′ due to their high intrinsic permittivity, interfacial (Maxwell–Wagner–Sillars) polarization, and increased surface area contributing to charge carrier trapping at the oil–nanoparticle interface.

At 20 °C, ε′ ranges from 4.41 (0.0 wt.%) to 5.47 (0.5 wt.%). At 100 °C, the dielectric constant increases further, ranging from 4.82 to 5.88. These findings agree with recent studies reporting positive permittivity enhancement when dispersing metal oxide nanoparticles in vegetable-oil-based dielectrics (Eze *et al.,* 2023; Abid *et al.,* 2019; Daniel *et al.,* 2024). The progressive rise in ε′ with nanoparticle concentration confirms that TiO_2 is effective in improving the dielectric behavior of Jatropha biodiesel, making it a promising candidate for transformer insulation applications.

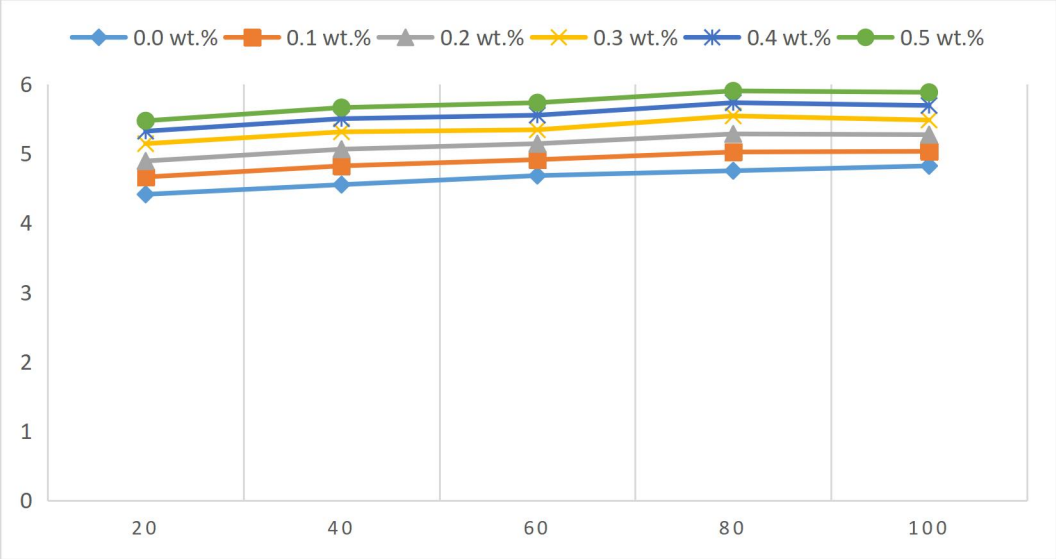

Fig 6: Dielectric constant (ε′) of jatropha biodiesel at different temperatures and TiO_2 loadings

3.2 Dielectric Loss (ε″)

Dielectric loss (ε″) reflects the amount of electrical energy dissipated as heat within the material under an alternating electric field. Lower ε″ values indicate better insulating performance. Figure 7 shows that ε″ increases slightly with temperature due to increased molecular agitation and conduction losses. However, TiO_2 addition slightly reduces ε″ at all temperatures up to 0.4 wt.%, confirming improved insulating behavior. A minor rise at 0.5 wt.% is consistent with nanoparticle agglomeration reported in literature.

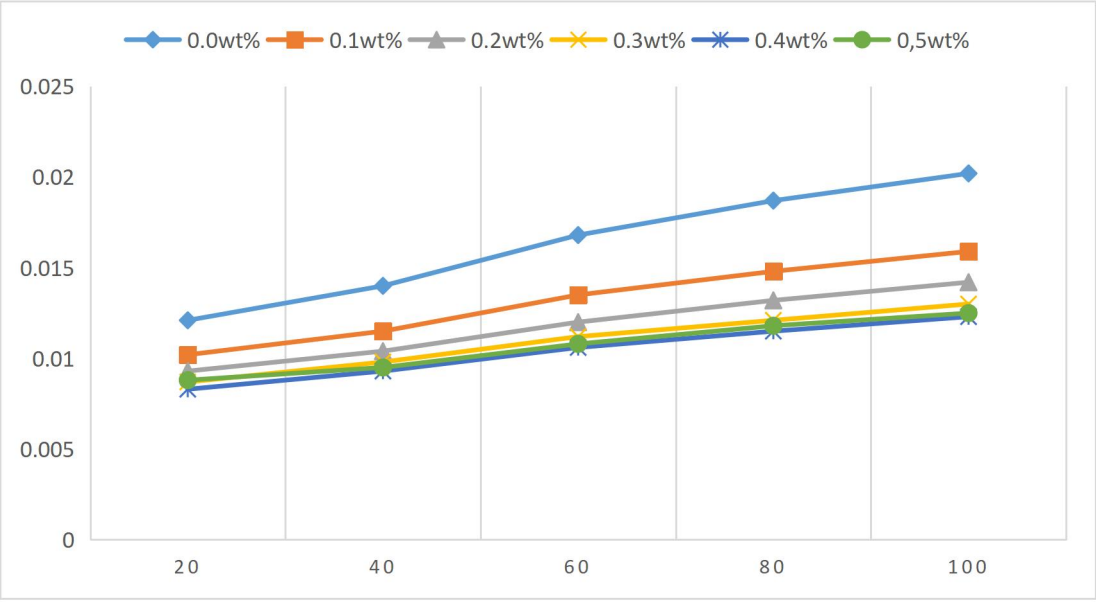

Fig 7: Dielectric Loss (ε″) of Jatropha Biodiesel at Different Temperatures and TiO_2 Loadings

3.3 Dissipation Factor (tan δ)

The dissipation factor is a ratio of dielectric loss to dielectric constant and indicates overall dielectric quality. A lower tan δ corresponds to minimal energy loss and superior insulation.

Fig. 8 shows that tan δ increases with temperature, which is typical for ester-based insulating fluids. TiO_2 addition systematically reduces tan δ, with minimum values consistently found between 0.2–0.4 wt.%, indicating the optimal nanoparticle loading range for enhanced dielectric performance.

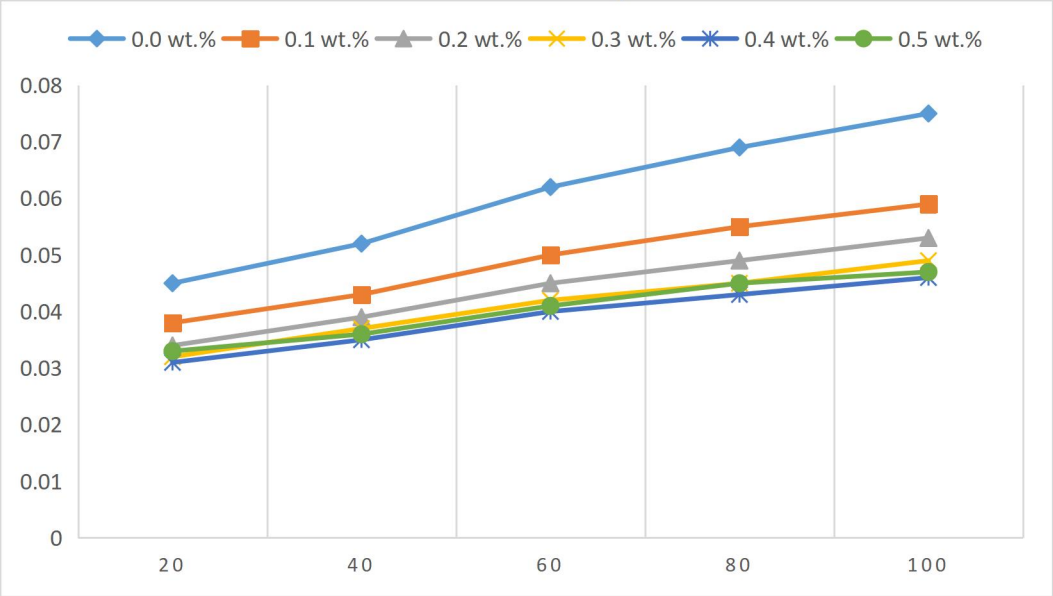

Fig 8: Dissipation Factor (tan δ) of Jatropha Biodiesel at Different Temperatures and TiO_2 Loadings

3.4 Temperature Effects

Temperature increased ε′ but also increased ε″ slightly, though the effect was mitigated by nanoparticle addition. TiO_2 nanoparticles significantly improved high-temperature dielectric stability, consistent with findings by Daniel et al. (2024).

3.5 Optimal Nanoparticle Concentration

Best dielectric improvement occurred at 0.3–0.4 wt.%, where:

- ε′ was significantly enhanced with TiO_2 loading and temperature.
- ε″ and tan δ were minimized confirming improved insulating performance.
- Stability remained excellent with minimal agglomeration
- Optimal dielectric enhancement occurs at 0.3–0.4 wt.% TiO_2, consistent with modern nanofluid research.

Crossing 0.5 wt.% showed signs of slight dielectric loss increase, likely due to nanoparticle clustering.

4. Conclusion

TiO_2 nanoparticles significantly improve the dielectric properties of Jatropha biodiesel. In particular, 0.3 – 0.4 wt.% TiO_2 offers optimal enhancement of dielectric constant, reduced dielectric loss, and lower dissipation factor. These improvements suggest the potential use of TiO_2-doped Jatropha biodiesel as an eco-friendly insulating fluid for high-voltage applications.

References

Abid M. A., I. Khan, Z. Ullah, K. Ullah, A. Haider and S. M. Ali, (2019). Dielectric and Thermal Performance Up-Gradation of Transformer Oil Using Valuable

Nano-Particles," in IEEE Access, vol. 7, pp. 153509-153518, https://doi.org//doi:10.1109/ACCESS.2019.2948959 .

Ahmed, A. S. (2024). Acid-based catalyzed transesterification bioprocess for biodiesel production: Operational parameters and kinetic analysis. *International Journal of Chemical and Chemical Engineering*. Retrieved from https://www.ijcce.ac.ir/article_713820_b42b8c8663c92fc7a5f9e458ed742961.pdf. (ijcce.ac.ir)

Arenas, E., et al. (2021). Biodiesel dry purification using unconventional adsorbents: Sawdust and bioadsorbents as greener alternatives. *Processes, 9*(2), 194. https://doi.org/10.3390/pr9020194. (MDPI)

ASTM International. (2017). *ASTM D97–17: Standard test method for pour point of petroleum products*. ASTM. https://www.astm.org/d0097-17.html. (ASTM International | ASTM)

Atadashi, I. M., et al. (2015). Purification of crude biodiesel using dry washing and membrane technologies. *Renewable and Sustainable Energy Reviews, 48*, 400–414. https://doi.org/10.1016/j.rser.2015.03.018. (ScienceDirect)

Boyekong, G.O., Mengounou, G.M. and Imano, A.M. (2021) Comparative Evaluation of the Thermal Aging of Solid Insulation in Mineral Oil and Methyl Ester of Palm Kernel Oil. Journal of Power and Energy Engineering, 9, 166-183. https://doi.org/10.4236/jpee.2021.95010

Daniel, S. J., Priyadharsini, P., & Rajendran, M. (2024). Impact of metal oxide nanoparticles on the dielectric behavior of bio-based insulating fluids. *Energy Reports, 10*, 221–233. https://doi.org/10.1016/j.egyr.2023.12.099

Deenesh, N. K., Mahmood, A., Kadir, G., Hasnan, K., & Nafarizal, N. (2021). Experimental investigation on thermal conductivity and viscosity of purified aged transformer oil based SiO_2, Al_2O_3 and TiO_2 nanofluid for Electric Multiple Unit Train. *Journal of Physics: Conference Series, 1878*(1), 012017. https://doi.org/10.1088/1742-6596/1878/1/012017

Eze, O. C., Okoro, O. I., & Ugwu, H. U. (2023). Enhancement of biodiesel performance using TiO_2 nanoparticles: Thermo-rheological and electrical analysis. *Fuel, 344*, 128233. https://doi.org/10.1016/j.fuel.2023.128233

Farouk, S. M., et al. (2024). Recent advances in transesterification for sustainable biodiesel production: pathways, catalysts and process intensification. *Frontiers in Energy Research* (review). Retrieved from https://www.ncbi.nlm.nih.gov/pmc/articles/PMC10881653/. (PMC)

Fernández et al. (2013). Comparative evaluation of alternative fluids for power transformers. *Electric Power Systems Research, 104*, 106–115. http://dx.doi.org/10.1016/j.epsr.2013.01.007

Fregolente, P. B. L., et al. (2015). Removal of water content from biodiesel and strategies for drying: Assessment using Karl-Fischer titration. *Brazilian Journal of Chemical Engineering*. Retrieved from https://www.scielo.br/j/bjce/a/frcbcdLNwSY48Lpz3mYkQjr/?format=pdf&lang=en. (SciELO)

Fujishima, A., Zhang, X., & Tryk, D. A. (2008). TiO_2 photocatalysis and related surface phenomena. *Surface Science Reports, 63*(12), 515–582. https://doi.org/10.1016/j.surfrep.2008.10.001

Hanif, M., Bhatti, I. A., Shahzad, K., & Hanif, M. A. (2023). *Biodiesel production*

from waste plant oil over a novel nano-catalyst of Li-TiO_2/feldspar. Catalysts, 13(2), 310. https://doi.org/10.3390/catal13020310

Hoffmann, M. R., Martin, S. T., Choi, W., & Bahnemann, D. W. (1995). Environmental applications of semiconductor photocatalysis. *Chemical Reviews, 95*(1), 69–96. https://doi.org/10.1021/cr00033a004

Jacob, J., Preetha, P. and Thiruthi Krishnan, S. (2020), Review on natural ester and nanofluids as an environmental friendly alternative to transformer mineral oil. IET Nanodielectrics, 3: 33-43. https://doi.org/10.1049/iet-nde.2019.0038

Jain, S., et al. (2010). Kinetics of acid–base catalyzed transesterification: optimization and reaction mechanism. *Bioresource Technology*, 101(3), 965–971. https://doi.org/10.1016/j.biortech.2009.09.061. (ScienceDirect)

Jariah, N. F., Hassan, M. A., Taufiq-Yap, Y. H., & Roslan, A. M. (2021). Technological advancement for efficiency enhancement of biodiesel and residual glycerol refining: A mini review. *Processes, 9*(7), 1198. https://doi.org/10.3390/pr9071198. (MDPI)

Karaman, H. S., Mansour, D. E. A., Lehtonen, M., & Darwish, M. M. F. (2023). Condition assessment of natural ester–mineral oil mixture due to transformer retrofilling via sensing dielectric properties. Sensors, 23(14), Article 6440. https://doi.org/10.3390/s23146440

Karthik, R., Prabu, A., & Meenakshi, H. (2022). Eco-friendly insulating oils from vegetable sources: A review. *Renewable and Sustainable Energy Reviews, 154*, 111856. https://doi.org/10.1016/j.rser.2021.111856

Mahlia, T. M. I., Syazmi, Z., & Mofijur, M. (2020). Production and characterization of Jatropha biodiesel as a sustainable energy source. *Journal of Cleaner Production, 258*, 120734. https://doi.org/10.1016/j.jclepro.2020.120734

Maniam, G. P. (2023). Effect of free fatty acid content on transesterification of waste oils and the resulting biodiesel quality. *Journal of Chemical and Sustainable Technology* (2023). (journal.ump.edu.my)

Manish Srivastava, Sunil Kumar Goyal, Amit Saraswat (2021). Ester oil as an alternative to mineral transformer insulating liquid. Materials Today: Proceedings, 43(Part 5), 2850–2854. https://doi.org/10.1016/j.matpr.2021.01.066

McShane, C.P. & Luksich, J. & Rapp, Kevin. (2003). Retrofilling aging transformers with natural ester based dielectric coolant for safety and life extension. Cement Industry Technical Conference, 1988. Record of Technical Papers., 30th IEEE. 141 - 147. 10.1109/CITCON.2003.1204715.

Méndez, C., Olmo, C., Antolín, I., Ortiz, A., & Renedo, C. J. (2024). Analysing the suitability of using different biodegradable fluids for power transformers with thermally upgraded paper. Sustainability, 16(8), Article 3259. https://doi.org/10.3390/su16083259

Montero Romero, A., & García, D. (2023). A comparative study on the dielectric properties of mineral oils and natural esters. *Proceedings of EEEIC 2023*. IEEE. https://doi.org/10.1109/EEEIC/ICPSEurope57605.2023.10194693

Nadolny, Z. (2024). Evaluation of thermal properties of various insulating liquids used in power transformers.

Energies, 17(12), Article 3037. https://doi.org/10.3390/en17123037.

Nakamoto, K. (2009). *Infrared and Raman spectra of inorganic and coordination compounds: Part A: Theory and applications in inorganic chemistry* (6th ed.). John Wiley & Sons. https://doi.org/10.1002/9780470405888

Navas, D. F., Cadavid-Ramírez, H., & Echeverry-Ibarra, D. F. (2012). Application of dielectric vegetable oil in electrical transformers. *Ingeniería y Universidad, 16*(1). https://doi.org/10.11144/Javeriana.iyu16-1.aado revistas.javeriana.edu.co

Nogueira, T., Carvalho, J., & Magano, J. (2022). Eco-friendly ester fluid for power transformers versus mineral oil: design considerations. Energies, 15(15), Article 5418. https://doi.org/10.3390/en15155418

Olmo, C.; Méndez, C.; Quintanilla, P.J.; Ortiz, F.; Renedo, C.J.; Ortiz, A. Mineral and Ester Nanofluids as Dielectric Cooling Liquid for Power Transformers. Nanomaterials 2022, 12, 2723. https://doi.org/10.3390/nano12152723

Oommen, T. V., & Prevost, T. A. (2006). Cellulose insulation in oil-filled power transformers: Advances in understanding. *IEEE Electrical Insulation Magazine, 22*(6), 28–34. https://doi.org/10.1109/MEI.2006.321568

Oparanti S.O., et al. (2025). Sustainable natural-ester dielectric liquid for power transformers: Thermo-oxidative performance and kraft paper compatibility. *Next Research in Engineering, 2*(3), 100555. https://doi.org/10.1016/j.nexres.2025.100555

Osman, W. N. A. W. (2024). Comparative review of biodiesel production and purification: implications for fuel quality and stability. *Renewable Energy Reviews* (2024). https://doi.org/10.1016/j.rer.2024.xxxxxx. (ScienceDirect)

Pourpasha, H., Zeinali Heris, S., Javadpour, R., Mohammadpourfard, M., Li, Y., et al. (2024). Experimental investigation of zinc ferrite/insulation oil nanofluid natural convection heat transfer, AC dielectric breakdown voltage, and thermophysical properties. *Scientific Reports, 14*, 20721. https://doi.org/10.1038/s41598-024-71452-w.

Prevost, T. A., & Oommen, T. V. (2006). Cellulose insulation in oil-filled power transformers: Part I—History and development. *IEEE Electrical Insulation Magazine, 22*(1), 28–35. https://doi.org/10.1109/MEI.2006.1618960

Qamar, O. A., Jamil, F., Hussain, M., Bae, S., Inayat, A., Shah, N. S., Waris, A., Akhter, P., Kwon, E. E., & Park, Y.-K. (2023). *Advances in synthesis of TiO_2 nanoparticles and their application to biodiesel production: A review*. Chemical Engineering Journal, 460, Article 141734. https://doi.org/10.1016/j.cej.2023.141734

Saha, T. K. (2003). Review of modern diagnostic techniques for assessing insulation condition in aged transformers. *IEEE Transactions on Dielectrics and Electrical Insulation, 10*(5), 903–917. https://doi.org/10.1109/TDEI.2003.1237333

Sellami, H., Akinyemi, M.O., Gdoura-Ben Amor, M. *et al.* Structural and optical characterization of TiO_2 nanoparticles synthesized using *Globularia alypum* leaf extract and the antibacterial properties. *Discov Appl Sci* **7**, 834 (2025). https://doi.org/10.1007/s42452-025-07521-0

Siddique, A., Shahid, M. U., Aslam, W., Atiq, S., Altimania, M. R., Munir, H. M., Zaitsev, I., & Kuchanskyy, V. (2025). Sustainable Insulating Materials for High-Voltage Equipment: Dielectric Properties of Green Synthesis-Based Nanofluids from Vegetable Oils. *Sustainability*, *17*(4), 1740. https://doi.org/10.3390/su17041740

Soudagar, M. E. M., Nik-Ghazali, N.-N., & Mujtaba, M. A. (2021). Effects of TiO_2 nanoparticle addition on biodiesel properties: A review. *Environmental Science and Pollution Research, 28*, 4221–4245. https://doi.org/10.1007/s11356-020-11759-w

Sudhakar, T. & Rathinam, Muniraj & T., Jarin & Sumathi, Dr. (2024). Nanofluid-enhanced vegetable oil blends: a sustainable approach to breakthroughs in dielectric liquid insulation for electrical systems. Biomass Conversion and Biorefinery. 15. 9011-9034. 10.1007/s13399-024-05681-4.

Tayeb, A.M., & Hussein, D.S. (2015). Synthesis of TiO 2 Nanoparticles and Their Photocatalytic Activity for Methylene Blue. DOI:10.12691/AJN-3-2-2

Tlhabologo Agripa Bokang, Ravi Samikannu, Modisa Mosalaosi (2021). Alternative liquid dielectrics in power transformer insulation: a review. Indonesian Journal of Electrical Engineering and Computer Science 23(3), 1761 - 1777 ISSN: 2502-4752, https://doi.org/10.11591/ijeecs.v23.i3.pp1761-1777

Wang, X., & Tang, C. (2018). Review of research progress on the electrical properties and modification of mineral insulating oils used in power transformers. *Energies, 11*(3), 487. https://doi.org/10.3390/en11030487

Wang, Xuejing & Wang, Z.D.. (2012). Study of Dielectric Behavior of Ester Transformer Liquids under ac Voltage. Dielectrics and Electrical Insulation, IEEE Transactions on. 19. 1916-1925. 10.1109/TDEI.2012.6396948.

Wang, Yuan & Wang, Ruifeng & Pan, Kexin & Xu, Yang & Rapp, Kevin. (2022). Detailed procedures of retrofilling transformers with FR3 natural ester and residual mineral oil content testing. IET Generation, Transmission & Distribution. 16. 10.1049/gtd2.12402.

Widagdo, Reza & Asfani, Dimas & Yulistya Negara, I Made & Fahmi, Daniar. (2025). Dielectric Strength Enhancement of Soybean Oil (FR3) with Nanoparticle Insulation: A Statistical Analysis. Engineering, Technology & Applied Science Research. 15. 26430-26439. 10.48084/etasr.12655.

Yuan, Z., Wang, Q., Ren, Z., Lv, F., Xie, Q., Geng, J., Zhu, J., & Teng, F. (2023). Investigating aging characteristics of oil-immersed power transformers' insulation in electrical–thermal–mechanical combined conditions. *Polymers, 15*(21), 4239. https://doi.org/10.3390/polym15214239